

Studies on SLS Doped Polyaniline and Its Blend with PC

T. JEEVANANDA,¹ SIDDARAMAIAH,¹ V. ANNADURAI,² R. SOMASHEKAR²

¹ Department of Polymer Science and Technology, S. J. College of Engineering, Mysore 570 006, India

² Department of Studies in Physics, University of Mysore, Mysore 570 006, India

Received 14 March 2000; accepted 30 October 2000

ABSTRACT: Electrically conductive polyaniline (PANI) and its blend with polycarbonate (PC) was prepared by one-step emulsion polymerization technique in which sodium lauryl sulfate (SLS) acts as surfactant and as a protonating agent for the resulting polymer. The prepared PANI and its blends were characterized by density, percentage of water absorption, and electrical conductivity. PANI-PC blend exhibits a conductivity value of 4.70×10^{-2} S/cm (PANI-PC1) and 5.68×10^{-5} S/cm (PANI-PC3) with a change in dopant from *p*-toluene sulfonic acid (TSA) to SLS, respectively. By using a more general method, which takes into account the presence of disorder of the second kind in polymers proposed by Hosemann, crystal size ($\langle N \rangle$) and lattice strain (g in %) values were estimated. The variation of conductivity in doped PANI and PANI-PC blend has been explained on the basis of these microcrystalline parameters. TGA thermograms of PANI and PANI-PC blend show three-step degradation behavior. Thermal stability of PANI was improved after blending with PC. © 2001 John Wiley & Sons, Inc. *J Appl Polym Sci* 82: 383–388, 2001

Key words: polyaniline; polycarbonate; electrical conductivity; WAXS

INTRODUCTION

Polyaniline (PANI), one of the oldest conducting polymers, is under extensive study even today because of its high environmental stability, low cost, and simple synthesizing procedures.^{1–3} It has potential applications in light-emitting diodes (LED), batteries, electromagnetic shielding, gas sensors, and antistatic and anticorrosion agents.^{4–9} The conductivity of PANI is very much dependent on the protonating agent and protonation level and varies from 10^{-12} to 10 S/cm between undoped and doped states.¹⁰ PANI doped with inorganic anions such as Cl^{-1} or ClO_4^{-1} will give good conductivity, but

readily undergoes partial undoping when immersed in water due to the migration of the anion out of the polymer network.¹¹ The solubility and stability of PANI can be improved by using functionalized protonic acids such as dodecylbenzene sulfonic acid (DBSA),^{12,13} dodecyl sulfuric acid (DSA),¹⁴ sulfosalicylic acid (SSA),¹⁵ camphor sulfonic acid (CSA),¹⁶ *p*-toluene sulfonic acid (TSA),¹⁷ and phosphoric acid esters.^{18–20} The processibility of polyaniline can be improved by preparation of composites with commercial polymers. Ruckenstein and Yang^{21,22} reported a method for the preparation of PANI composites with polystyrene and poly(alkyl methacrylate). Recently, Jeon et al.²³ prepared polyaniline-polycarbonate (PANI-PC) composites by using DBSA as surfactant and dopant. The above articles do not deal with the structural–property relationship of PANI and its blend/composite in detail.

The objective is to produce a conductive blend that maintains the mechanical properties, the

Correspondence to: Siddaramaiah (siddaramaiah@yahoo.com).

Contract grant sponsor: CSIR; contract grant number: 8/452 (1)/2000, EMR-I-SPS.

Journal of Applied Polymer Science, Vol. 82, 383–388 (2001)
© 2001 John Wiley & Sons, Inc.

processibility, and the thermal stability of conventional polymers, together with the electrical properties of conducting PANI. In this article, we have attempted to prepare PANI and its blend with polycarbonate (PC) in chloroform by one-step emulsion polymerization technique. The engineering plastic PC has been selected as a polymer matrix for its good mechanical strength and good dimensional and thermal stability. We have also tried to prepare PANI and its blend by using benzoyl peroxide (BPO) as an initiator. Some of its physical, electrical, and thermal properties are reported. The variation of electrical conductivity with microcrystalline parameters was carried out by wide-angle X-ray scattering (WAXS) studies.

EXPERIMENTAL

Materials

Aniline was vacuum distilled under nitrogen prior to use. Reagent-grade sodium lauryl sulfate (SLS), TSA, chloroform, ammonium persulfate (APS), and BPO (E. Merck, India) were used as purchased. PC (density, 1.2 g/cc³ and conductivity > 10⁻¹² S/cm) was obtained from M/s. G.E. Plastics, India.

Preparation of PANI

Emulsion polymerization of aniline in chloroform was carried out by using SLS, which was employed as surfactant and also as a dopant. Polymerization was initiated by the addition of an aqueous solution of APS (aniline-to-APS molar ratio 1 : 1) over a period of 30 min to avoid exothermic reaction. The reaction was carried out at room temperature, because below room temperature the viscosity was high. The emulsion was stirred for 24 h and the polymerization was terminated by pouring the resulting highly viscous emulsion into acetone. The dark-green powder was extensively washed with 2–3 L of distilled water to remove excess dopant and APS. Finally, it was washed with acetone to remove water. The powder was dried in a desiccator for 48 h. The obtained PANI was soluble in chloroform.

The prepared PANI was characterized by electronic absorption spectra on Shimadzu UV/Visible spectrophotometer in chloroform solvent. The emeraldine salt form exhibits three distinct absorption peaks: an absorption peak at 350 nm corresponding to a π - π^* transition of the benze-

Table I Sample Code for PANI and PANI-PC (35/65) Blends

Sample Code	Composition	Oxidant	Dopant
PANI	100/0	APS	SLS
PANI1	100/0	BPO	SLS
PANI-PC1	35/65	APS	<i>p</i> -TSA
PANI-PC2	35/65	BPO	<i>p</i> -TSA
PANI-PC3	35/65	APS	SLS
PANI-PC4	35/65	BPO	SLS

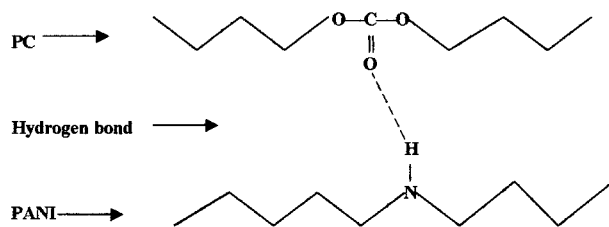
APS, ammonium persulfate; SLS, sodium lauryl sulfate; BPO, benzoyl peroxide; *p*-TSA, *p*-toluene sulfonic acid.

noid ring and two absorption peaks at 430 and 820 nm which can be assigned to the polaron band transitions.²⁴

Preparation of PANI-PC Blend

The PANI-PC blends were prepared by starting from an emulsion in which an aqueous solution of SLS constitutes the continuous phase and a chloroform solution of aniline and PC constitutes the dispersed phase. In a typical experiment, 5.25 g of PC was dissolved in 100 mL of chloroform in a 500-mL flask with 2.3 mL (0.25M) aniline. To this, 50 mL of aqueous solution containing 2.88 g (0.2M) of SLS was added dropwise with stirring. Then, 100 mL of 0.25M *p*-toluene sulfonic acid/SLS aqueous solution containing 5.7 g (0.25M) of APS were introduced dropwise with stirring to polymerize the aniline and dope the PANI-PC blend. The emulsion was stirred for 24 h at room temperature. The polymerization was terminated by pouring the resulting highly viscous emulsion into acetone. The dark-green powder was extensively washed with 2–3 L of distilled water to remove excess of dopant and APS. Finally, it was washed with acetone to remove water. The powder was dried in a desiccator for 48 h. The above procedure is similar to the one that is reported in the literature.²¹ The sample codes used for prepared PANI and PANI-PC blends are given in Table I.

FTIR spectra of PANI-PC blend was recorded by using a Perkin-Elmer Model 2000 FTIR instrument employing the KBr pellet technique. The IR spectra of the PANI-PC blend shows two absorption peaks: one at 1776 cm⁻¹ is due to carbonyl-stretching region of PC and another at 1770 cm⁻¹ is caused by the hydrogen bonding between —C=O of PC and —NH of PANI (shown in Scheme 1).²⁵



Scheme 1 Hydrogen bond between PANI and PC.

Characterization

Physical properties, such as density and percentage of water absorption, were measured as per ASTM D792-86 and ASTM D570, respectively. The powder was shaped into a disk (2.5 cm diameter \times 0.1 cm thick) at an applied pressure of 120 MPa at room temperature. The standard four-probe method was employed to measure the electrical conductivity of the disks. The TGA thermograms were obtained by using a DuPont 2000 thermal analyzer from ambient to 800°C at a scanning rate of 10°C/min in air atmosphere.

X-ray Recording and Profile Analysis

X-ray diffraction data on powder samples were collected on a STOE/STADIP X-ray powder diffractometer with germanium monochromated $\text{CuK}\alpha$ ($\lambda = 1.5406 \text{ \AA}$) radiation in a transmission mode, using a curved position sensitive detector (CPSD) in the 2θ range from 5 to 53° at step sizes of 0.03°. The trial and error indexing program (TREOR)²⁶ was used in determining the unit cell parameters. All these samples belong to the orthorhombic system and the lattice parameters are $a = 8.566$, $b = 8.566$, and $c = 23.169$ in \AA . X-ray diffractograms of all the samples are given in Figure 1(a–d). It is evident from Figure 1(a–d) that there is a broadening which arises due to two main factors. According to Warren,²⁷ these are due to a decrease in (i) crystal size (N) and a increase in (ii) strain (lattice disorder) (g in %) present in the samples.

We have estimated these parameters by simulating the profile by employing the procedure described earlier^{28–32} and by using Bragg reflection at $2\theta = 24.9^\circ$. The following equations have been used to simulate X-ray reflection:

$$I(s) = I_{N-1}(s) + I'_N(s) \quad (1)$$

where

$$I_N(s) = 2 \times \text{Re} \left(\frac{(1 - I^{N+1})}{(1 - I)} + \frac{Iv}{d(1 - I)^2} \right)^{-1} \times \{I^N(N(1 - I) + 1) - 1\} \quad (2)$$

where

$$v = 2ia^2s + d \text{ and } I = I_1(s) \\ = \exp(-a^2s^2 + ids); a^2 = \omega^2/2 \quad (3)$$

Also,

$$I'_N(s) = \frac{2\alpha_N}{D(\pi)^{1/2}} \exp(iDs) (1 - \alpha_N s \{2D(\alpha_N s) \\ + i(\pi)^{1/2} \exp(-\alpha_N^2 s^2)\}) \quad (4)$$

with $\alpha_N^2 = N\omega^2/2$, where ω is the standard deviation of the nearest neighbor probability function, $D(\alpha_N s)$ is the Dawson's integral or the error function with complex argument and can be computed. $\langle N \rangle$ is the number of unit cells counted in a direction perpendicular to the (hkl) Bragg plane,

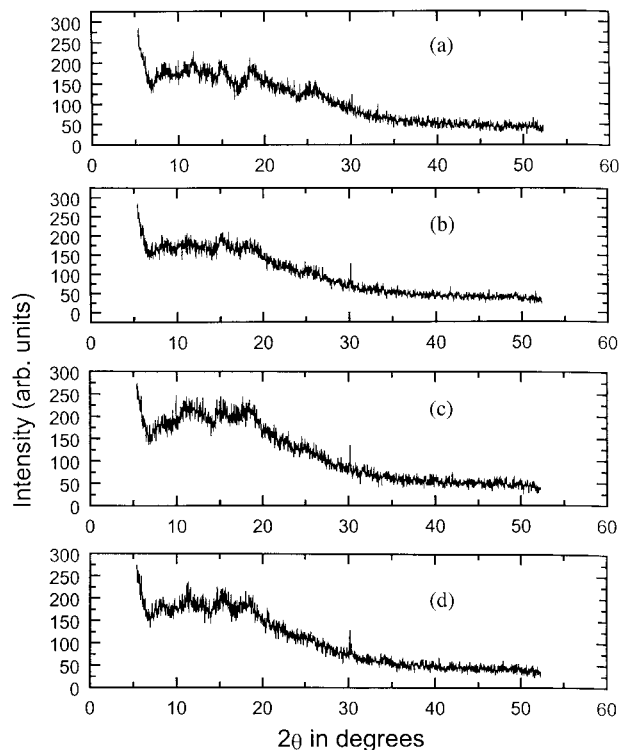


Figure 1 Wide-angle X-ray scattering patterns for the samples (a) PANI, (b) PANI-PC1, (c) PANI-PC2, and (d) PANI-PC3.

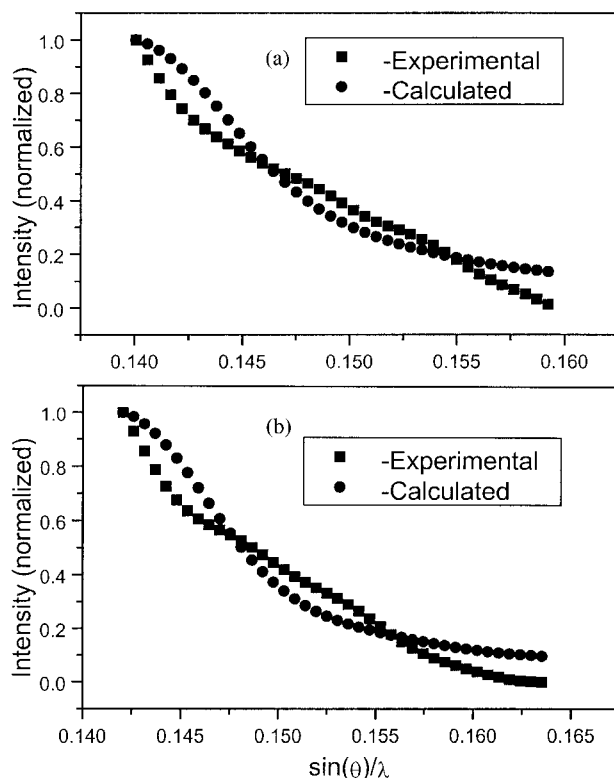


Figure 2 Experimental and simulated X-ray profile for the samples (a) PANI-PC1 and (b) PANI-PC3.

d is the spacing of the (hkl) planes, Re refers to the real part of the expression, s is $\sin\theta/\lambda$, λ is the wavelength of X-rays used, a is related to the standard deviation ω of lattice distribution function, and D is the crystal size ($=\langle N \rangle d_{hkl}$). $I_N'(s)$ is the modified intensity for the probability peak centered at D .

For the sake of completeness we have reproduced in Figure 2(a, b), the simulated and experimental profiles for the samples (a) PANI-PC1 and (b) PANI-PC3. In fact, the goodness of the fit was $< 2\%$ in all the samples.

RESULTS AND DISCUSSION

The measured properties such as density, percentage of water absorption, and electrical conductivity values are presented in Table II. From Table II, it is evident that the density and percentage of water absorption are high for PANI when compared to PANI-PC blends. This is due to the density percent water absorption of PC being less than that of PANI.

PANI-PC blends were prepared by using different dopant and oxidant combinations. From Table II, it can be noted that changes are observed in density and percentage of water absorption for all PANI-PC blends. PANI-PC blend prepared by using APS and *p*-TSA as an oxidant and dopant, respectively, shows maximum conductivity (PANI-PC1), whereas conductivity has a low value for APS and SLS combination (PANI-PC3). This is due to poor doping power of SLS compared to *p*-TSA. PANI was not formed when BPO and SLS were used as oxidant and dopant, respectively. This may be due to the poor oxidation power of BPO at room temperature.

The X-ray equatorial recordings in Figure 1, which consist of one intense broad reflection at 24.9° , categorically suggest that the diffraction is by an amorphous polymer and is almost equivalent to the insulating emeraldine base state observed in PANI.^{33–35} Earlier, computation of crystal size in PANI was carried out by using the Scherrer equation and it has been stated that the value ranges from 30 to 70 Å. It is also mentioned that these values are a crude estimation, as other effects have not been considered. Table III gives the various microcrystalline parameters such as crystal size ($\langle N \rangle$), smallest crystal unit (p), crystal size distribution (α), lattice strain (g), and enthalpy (α^*). In this study, we have estimated both crystal size ($\langle N \rangle$) and lattice strain (g in %) by using a more general Hosemann's paracrystalline method,³⁶ which takes into account the presence of disorder of a second kind. In fact, broadening of reflections arises mainly due to these two effects. The crystal size value in the present case is on the order of 28 Å [$=\langle N \rangle d_{hkl}$]. It is also observed that these crystal-size and lattice-strain values change with dopants and oxidants

Table II Density, % of Water Absorption, and Electrical Conductivity Values of PANI and PANI-PC (35/65) Blends

Sample Code	Density (g/cc ³)	Water Absorption (%)	Conductivity (S/cm)
PANI	1.354	3.931	1.60×10^{-2}
PANI1 ^a	—	—	—
PANI-PC1	1.188	2.667	4.70×10^{-2}
PANI-PC2	1.177	2.266	2.72×10^{-2}
PANI-PC3	1.198	2.643	5.68×10^{-5}
PANI-PC4 ^b	—	—	—

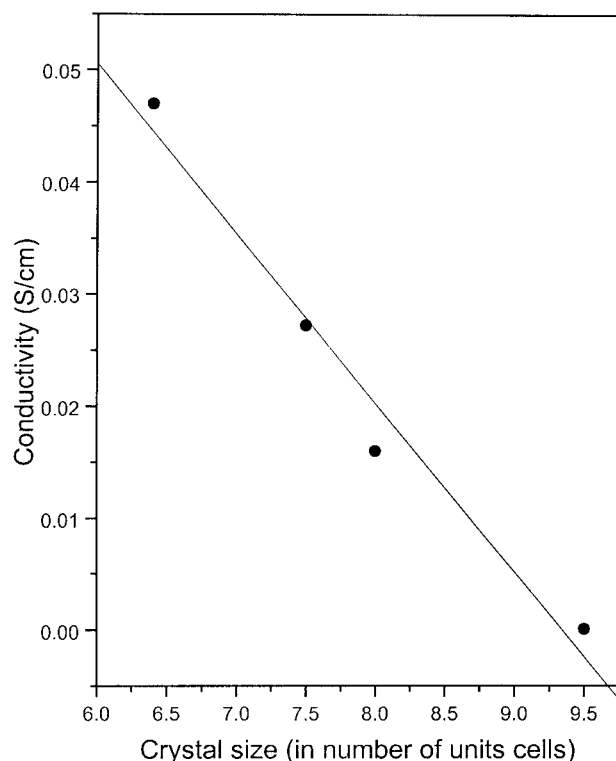
^a Does not form PANI.

^b Does not form PANI-PC blend.

Table III The Microcrystalline Parameters of PANI and PANI-PC (35/65) Blends Using Bragg Reflection Observed at $2\theta = 24.9^\circ$

Sample Code	$\langle N \rangle$	p	α	g in %	α^*
PANI	8.0 ± 0.1	4.20	0.263	7.5 ± 0.1	0.21
PANI-PC1	6.4 ± 0.1	3.74	0.385	9.4 ± 0.1	0.24
PANI-PC2	7.5 ± 0.1	4.11	0.295	8.3 ± 0.1	0.23
PANI-PC3	9.5 ± 0.1	9.28	4.983	10.4 ± 0.1	0.32

and hence the conductivity. From Figure 3, it is observed that a relatively high conductivity is observed in a blend having less crystal size and lattice strain values. This is consistent with earlier observations^{33–35} that the doped PANI has intrinsic in-chain conductivity. The lower conductivity reflects the presence of increased localization of charges and hence leads to changes in crystal-size values. In fact, variation of crystallinity both parallel and perpendicular to polymer chain direction leads to delocalization of charges and hence affects the conductivity values. Essentially this implies that with increase in regions of disorder in the polymer network, the conductivity associated with a free ion increases because of lower potential barrier.

**Figure 3** Variation of electrical conductivity with crystal size observed in PANI and PANI-PC blends.

It is evident from Table III that the enthalpy (α^*) values are < 0.32 and hence the parameter $\langle N \rangle$ corresponds to the crystal size.³⁶ Also, α^* remains constant for all the PANI-PC blends, indicating that the energy required for the formation of polymer network does not vary with the nature of dopant and oxidant. This minimum value of α^* indicates the phase stabilization of PANI-PC blends.

Thermal degradation characteristic behavior of PANI and PANI-PC blends were also studied and are given in Tables IV and V. PANI shows a three-step thermal degradation process in the temperature range 60–160, 160–345, and 345–660°C for moisture loss, dopant loss, and main-chain degradation of PANI, respectively.^{37,38} PANI-PC blends with different dopant and oxidant combinations also show three-step weight loss. The first step weight loss occurs in the range 95–400°C due to moisture and dopant loss; the second step in the range 320–500°C is due to PANI degradation. The third step is due to PC degradation and is in the range 500–750°C.

The relative thermal stability of the PANI and PANI-PC blends were evaluated by comparing decomposition temperatures at various percentage weight loss and are presented in Table V. From Table V, it was observed that the initial thermal stability of PANI is enhanced after blending with PC. This is due to the (i) hydrogen bond formation between $-\text{NH}$ of PANI and

Table IV Data Obtained from TGA Thermogram of PANI and PANI-PC (35/65) Blends

Sample Code	Degradation Temperature Range (°C)		
	First Step	Second Step	Third Step
PANI	60–160	160–345	345–660
PANI-PC1	110–325	325–500	500–750
PANI-PC2	100–320	320–500	500–710
PANI-PC3	95–400	400–500	500–700

Table V Characteristic Transition Temperatures Obtained from TGA Thermogram of PANI and PANI-PC (35/65) Blends

Sample Code	T_0 (°C)	T_{10} (°C)	T_{20} (°C)	T_{50} (°C)	T_{\max} (°C)
PANI	60	95	260	450	660
PANI-PC1	100	250	425	515	750
PANI-PC2	100	330	430	535	710
PANI-PC3	100	270	430	530	700

—C=O of PC and (ii) the thermal stability of PC is very much higher compared to PANI.

CONCLUSION

The following conclusions can be drawn from the aforesaid study. (i) Better conductivity was observed for *p*-TSA-doped PANI-PC blend compared to SLS doped blend. The reason for which a change is attributed to the increase of disorder in polymer network and this has been quantified in terms of microcrystalline parameters computed by using WAXS data. (ii) The thermal stability of PANI was improved after blending with PC. This was due to chemical interaction (hydrogen bond formation) between PANI and PC.

One of the authors (T. Jeevananda) thanks CSIR, New Delhi, India for an SRF fellowship (8/452 (1)/2000, EMR-I-SPS).

REFERENCES

- Mac Diarmid, A. G.; Epstein, A. J. in *Science and Applications of Conducting Polymers*; Salaneck, W. R., Clark, D. T., Samuelson E. J., Eds.; IOP Publishers: Bristol, U.K., 1991; p 117.
- Bredas, J. L.; Silbey, R., Eds., *Conjugated Polymers*; Kh Academic: Dordrecht, 1991.
- Chiang, J.-C.; Mac Diarmid, A. G. *Synth Met* 1986, 13, 1993.
- Parker, I. D. *J Appl Phys* 1994, 75, 1656.
- Matsunaga, T.; Daifuku, H.; Nakajima, T.; Kawagoe, T. *Polym Adv Tech* 1990, 1, 33.
- Bigg, D. M. *Adv Polym Tech* 1984, 4, 255.
- Sotomayor, M. P. T.; De Paoli, M.-A.; Oliveira, W. A. *Anal Chim Acta* 1997, 353, 275.
- Jeevananda, T.; Palaniappan, S.; Siddaramaiah, *J Appl Polym Sci* 1999, 74, 3507.
- Tsumura, A.; Fuchigami, H.; Koezuka, H. *Synth Met* 1991, 41–43, 1181.
- Zhao, B.; Neoh, K. G.; Liu, F. T.; Kang, E. T.; Tan, K. L. *Langmuir* 1999, 15, 8259.
- Neoh, K. G.; Kang, E. T.; Tan, K. L. *Polym Degrad Stab* 1994, 43, 141.
- Cao, Y.; Smith, P.; Heeger, A. J. *Synth Met* 1992, 48, 91.
- Osterholm, J. E.; Cao, Y.; Klavetter, F.; Smith, P. *Polymer* 1994, 35, 2902.
- Rathi, M.; Ponrathnam, S.; Rajan, C. R. *Macromol Rapid Commun* 1998, 19, 119.
- Tzou, K.; Gregory, R. V. *Synth Met* 1993, 53, 365.
- Cao, Y.; Smith, P. *Polymer* 1993, 34, 3139.
- Shacklette, L. W.; Han, C. C.; Luly, M. H. *Synth Met* 1993, 55–57, 3532.
- Pron, A.; Osterholm, J. E.; Smith, P.; Heeger, A. J.; Laska, J.; Zagorska, M. *Synth Met* 1993, 55–57, 3520.
- Pron, A.; Laska, J.; Osterholm, J. E.; Smith, P. *Polymer* 1993, 34, 4235.
- Laska, J.; Pron, A.; Lefrant, S. *J Polym Sci, Polym Chem Ed* 1995, 33, 1437.
- Ruckenstein, E.; Yang, S. *Synth Met* 1993, 53, 283.
- Yang, S.; Ruckenstein, E. *Synth Met* 1993, 59, 1.
- Jeon, B. H.; Kim, S.; Choi, M. H.; Chung, I. J. *Synth Met* 1999, 104, 95.
- Liu, F. L.; Wudl, F.; Nowak, M.; Heeger, A. J. *J Am Chem Soc* 1986, 108, 8311.
- Kalaycioglu, E.; Akbulut, U.; Toppare, L. *J Appl Polym Sci* 1996, 61, 1067.
- De Wolff, P. M. *J Appl Cryst* 1968, 1, 108.
- Warren, B. E. *Prog Met Phys* 1959, 8, 147.
- Somashekar, R.; Somashekarappa, H. *J Appl Cryst* 1997, 30, 147.
- Press, W.; Flannery, B. P.; Teuklosky, S.; Vetterling, W. T. *Numerical Recipes*; Cambridge Univ. Press: Cambridge, U.K., 1988; p 284.
- Somashekar, R.; Hall, I. H.; Carr, P. D. *J Appl Cryst* 1989, 22, 363.
- Hall, I. H.; Somashekar, R. *J Appl Cryst* 1991, 24, 1051.
- Silver, M., M.Sc. Thesis, UMIST, U.K., 1988.
- Pouget, J. P.; Jozefowicz, M. E.; Epstein, A. J.; Tang, X.; MacDiarmid, A. G. *Macromolecules* 1991, 24, 779.
- Maron, J.; Winokur, M. J.; Mattes, B. R. *Macromolecules* 1995, 28, 4475.
- Winokur, M. J.; Mates, B. R. *Macromolecules* 1998, 31, 8183.
- Hosemann, R. *Colloid Polym Sci* 1982, 260, 864.
- Boyle, A.; Penneau, J. F.; Genies, E. M.; Rieckel, C. J. *J Polym Sci, Polym Phys Ed* 1992, 30, 265.
- Gazotti, W. A.; De Paoli, Jr., M. A. *Synth Met* 1996, 80, 263.